Digital Discovery

ROYAL SOCIETY OF CHEMISTRY

PAPER

View Article Online
View Journal | View Issue

Cite this: *Digital Discovery*, 2023, **2**, 1733

Autonomous biomimetic solid dispensing using a dual-arm robotic manipulator†

Ying Jiang,[a] Hatem Fakhruldeen,[a] Gabriella Pizzuto,[a] Louis Longley,[a] Ai He,[ab] Tianwei Dai,[a] Rob Clowes,[a] Nicola Rankin[a] and Andrew I. Cooper *[a]

Automation and robotics have the potential to transform the landscape of chemistry and materials research. However, there are still many repetitive manual processes in the laboratory that are challenging to automate. Solid dispensing is a key technique that underpins chemistry and materials science. Conventionally, a scientist weighs samples using a spatula and balance. While there are commercial implementations that automate solid dispensing, these can be costly and the methods suffer from certain limitations in terms of breadth of application, scale, and accuracy. Here, we demonstrate an automated solid dispensing system that uses a highly dexterous dual-arm robotic manipulator. The system can transfer milligram up to gram quantities of solids in a bio-mimetic fashion, mimicking the way that a scientist uses a spatula and an analytical balance. The core of this automated system is the dual-arm robot coupled with a fuzzy logic control algorithm to select the appropriate motion parameters and to manipulate spatulas of various sizes to dispense solids. Our early results suggest that this weighing method could have improved generality across a wide range of solid materials, including solids that abrade or block solid dispensing units that have moving parts. The dual-arm robot is also significantly cheaper than most commercially available solid dispensing platforms. Experiments indicate that our platform can automatically dispense solids with an accuracy as low as 2 mg, with the added functionality of resetting and dispensing again if the sample weight exceeds a predefined tolerance.

Received 24th April 2023
Accepted 28th June 2023

DOI: 10.1039/d3dd00075c

rsc.li/digitaldiscovery

1 Introduction

Automation and robotics are central to the acceleration of chemistry and materials research, for example to speed up monotonous and time-consuming processes such as solid dispensing. The dispensing of solids is necessary for most chemistry, materials, and pharmaceutical research, and there have been a number of examples of automating this task using robotics and specialised solid-dispensing instruments.[1–5] Researchers can perform solid dispensing with high accuracy and precision, but in practice, manual errors are common, particularly when the number of samples to be weighed becomes large. For instance, mistakes can be made in terms of recording and labelling the weights of the samples. Solid dispensing is a general task in pharmaceutical research and development,[6] as well as other areas of science such as solid-state inorganic chemistry, where preparations often involve solid handling of reagents that cannot be dissolved in common solvents. For these reasons, a generalizable and relatively inexpensive automated solid dispensing platform would be a desirable tool for laboratory-based scientists, allowing them to focus more on mentally-stimulating tasks. Longer term, minimising the risk of exposure to chemicals is an additional potential benefit of automation.[1,3,6]

Several solid dispensing platforms are commercially available, such as Chemspeed GDU-S SWILE, GDU-Pfd, Quantos (Mettler Toledo) and Chronect XPR robotic solid dispensing systems.[3,7–9] These platforms all exploit gravity combined with some kind of mechanical agitation or force to transfer solids from a dosing head to the receiving container, although the precise dosing mechanism differs from instrument to instrument. The Chemspeed GDU-S SWILE dispenser combines a piston and a glass capillary tube with an internal measurement balance, and the dispensing precision is further verified using an external analytical balance.[3,7–9] This allows precise dispensing of very small quantities of material (100 μg to 100 mg). By contrast, the Chemspeed GDU-Pfd and Quantos (Mettler Toledo) devices both employ larger dosing heads with moving parts, and can deal with larger volumes of material. The Chemspeed system employs a crescent-shaped valve inside of the head with the ability to open and close the dispensing head to a specific size to control the flow of the solid material. The Quantos device is equipped with spiral metal impellers inside the dispensing head, which uses a rotary tapping motion to dispense the solid into the receiving

[a]*School of Chemistry, University of Liverpool, L69 3BX, UK. E-mail: ying.jiang@liverpool.ac.uk; Tel: +44 (0)7422505866*

[b]*School of Chemistry, Massachusetts Institute of Technology, MA 02139, USA. E-mail: aihe@mit.edu*

† Electronic supplementary information (ESI) available. See DOI: https://doi.org/10.1039/d3dd00075c

container.[7,9] In the case of the Chemspeed device, the balance is suspended and moves to the receiving container; by contrast, the Quantos device is static, and the receiving container is delivered to an analytical balance, either by hand, by using an automated carousel, or by using a robotic arm. The Chronect XPR robotic solid dispensing system[10] combines the same dispensing technology as the Quantos system, coupled with a six-axis single robotic arm to manipulate the dispensing head, thus completely automating the solid dispensing process for multiple solids, much as for the Chemspeed GDU-Pfd.

The Quantos device uses a self-adaptive algorithm that optimises the dosing process based on previous dispenses.[11,12] For the Chemspeed GDU-Pfd, the dosing parameters can be either manually or automatically selected under normal or automode.[7,9]

For these instruments to function well, they quite often require the pre-treatment for solids with large grains using methods such as grinding to avoid large particles from blocking the dispensing heads. Moreover, these instruments can sometimes struggle to dispense particles with high hardness, such as abrasive materials, and such materials can also reduce the lifetime of the dosing heads dramatically because they have moving parts. These factors can limit the range of solid materials that can be dispensed using these platforms, and impact the cost of operation in the case of abrasive solids. The consumables cost for different instruments can also vary considerably. In case of the Chemspeed SWILE, the glass capillaries used for dispensing are relatively inexpensive. For the Quantos device, the dosing heads are consumable items and they have a pre-programmed maximum number of usage cycles. They are also recommended to be paired with a single solid only,[7] which increases the running cost of this platform. The dosing head of the Chemspeed GDU-Pfd can be cleaned, disassembled, and reused several times before it needs to be replaced, but again it is ultimately a consumable.[7]

Here we demonstrate a new, generalised solution for dispensing a diverse array of solid materials with high accuracy. Unlike previous methods, we mimic the traditional human approach to dispensing solids using a spatula and an analytical balance. To do this, we use a dual-arm robot that can carry out multiple tasks such as using the spatula, opening and closing the analytical balance, and moving both weighed samples and 'hoppers' of the solids to be dispensed to and from the balance. We have used a dual-arm robot instead of a single-arm robot, as in the Chronect XPR robotic solid dispensing platform, because it increases the versatility of the platform. Our method also overcome the issue of dispensing head blockage by certain solids; there are no dispensing heads and no moving parts, other than the robot itself. The system can be used to dispense amounts as small as 20 ± 2 mg while also easily scaling to multiple grams of samples, simply by providing the robot with a variety of spatula sizes. This makes this approach suitable for a wide range of applications including materials research, pharmaceutical chemistry, process chemistry, formulations, *etc.* Moreover, because there are no moving parts or dispensing heads, this system can easily dispense material that comprise large particles or a mixture of particle sizes, as well as abrasive materials. There are also some materials that are less compatible with the system, such as highly deliquescent solids, which are generally challenging for automated platforms. Uniquely, the versatility of the two-armed robot allows dispensing to be restarted if solid is added beyond a predetermined threshold amount, thus allowing very high precision to be achieved, albeit at the expense of speed.

2 Method

Our method is inspired by manual solid dispensing methods; the dual-armed robot carries out steps that are very similar to a conventional manual weighing process, using a fuzzy logic controller to handle the solid dispensing. To better illustrate our method, we will first describe a typical manual solid dispensing technique. We then outline our experiment setup and automated robotic solid dispensing algorithm. Finally, the fuzzy logic controller is discussed.

2.1 Manual solid dispensing

A manual solid dispensing process, as performed by a researcher in the laboratory, can be summarized as follows. First, the researcher prepares the solid, if necessary – for example, breaking up any large particulates or agglomerated material. Second, the researcher scoops some amount of the solid using an appropriate spatula, typically gauging the target amount based on experience or knowledge; for example, based on the material's density. This material is then transferred into a container, such as a pre-weighed sample vial or weighing boat, and placed on an analytical balance. Once the balance reading has stabilized, the amount is recorded and then this process is repeated until the target weight is achieved. The scientist also has the option of starting again if the target weight is exceeded – that is, tipping out the weighed solid and restarting the weighing process – something that cannot be done with current commercially available solid dispensing platforms.

One important consideration for the chemist is the selection of the appropriate spatula size, which is chosen to match the amount of solid to be dispensed. The scientist also implements a natural feedback algorithm for dispensing; slower and more careful dispensing motions are used as the target weight is approached. All of these steps informed our the design of our robotic solid dispensing platform, as discussed below.

2.2 Experimental setup

Our solid dispensing method uses a two-armed, seven-degree-of-freedom robot. The robot dispenses solids primarily by manipulating the appropriately sized spatulas, scooping the solid from a hopper and then transferring the solid; the individual operations are illustrated in Fig. 1.

An ABB YuMi robot is selected due to its flexibility and ability to use a wide range of human tools and equipment such as vial racks, hoppers, spatula racks, and analytical balances. All equipment are placed within the robot's workspace. We use 10 ml sample vials,‡ and a matching size of sample rack. Three

‡ Agilent Technologies 5190-2285.

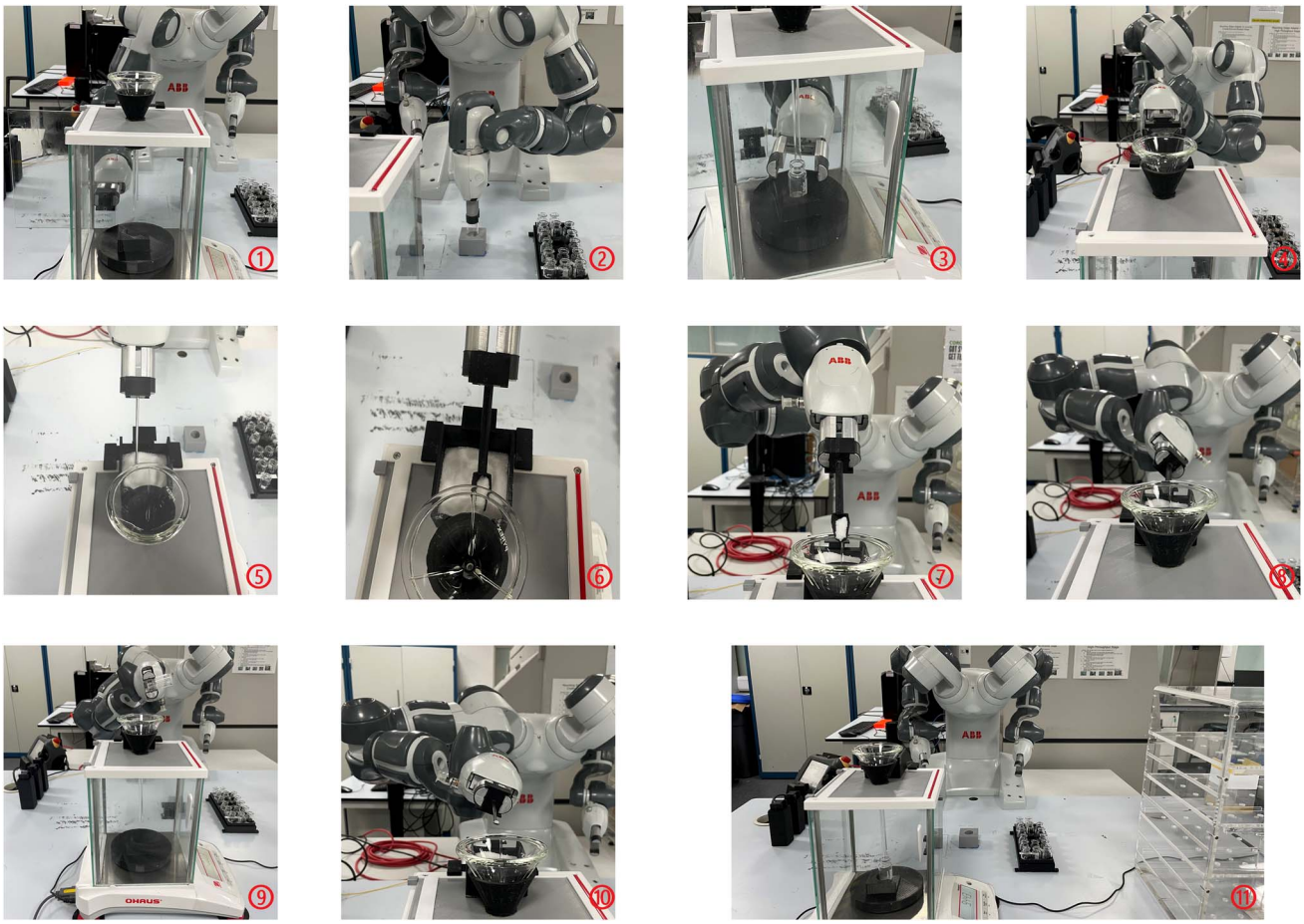

Fig. 1 Steps involved in automated solid dispensing using a dual-arm robot; (1) first, the robot opens the balance door; (2) and (3) the robot then manipulates the empty vial and places it on the analytical balance pan, before closing the balance door (not shown); (4) the robot manipulates the sample hopper that contains the material to be dispense, transferring it from a sample storage area (shown on right of image (11)), and placing it next to the balance; (5) the robot uses a small spatula to mix the contents of the hopper, breaking up any agglomerates; (6) the robot scoops solid from the sample hopper using a spatula that is matched in size to the amount to be dispensed; (7) photographs showing the tilting and shaking operations used to dispense the solids into a glass funnel that delivers the material to the sample vial; (8) any excess, undispensed solid is returned to the sample hopper; (9) tilting operation for smallest spatula; (10) here the robot removes the sample vial and returns all material to the sample hopper in the case of over-dispensing beyond a preset threshold (*i.e.*, a 'reset' operation); and (11) photograph showing the overall layout of the workflow. Videos of the solid dispensing process are provided in the Data availability section.

spatulas with different sizes are used for solid dispensing; these tools are stored between use in a vertical spatula holder rack.

Both the medium and large spatulas were designed§ to dispense 0.1 to 0.8 g¶ and more than 0.8 g, respectively. These spatulas were custom made and 3-D printed and are shown in Fig. 2. The spatula heads have enough depth to avoid the spillage of the solid material during transportation and each spatula has the same handle that is designed for easy and robust robot grasping. The front view of the medium and large spatulas is an inverted triangle and this allows the solids to be delivered precisely from the front of the spatula. For the smallest spatula, the solid is delivered from the side. The smallest spoon is designed for amounts of solid lower than 0.1 g, and is hemispherical. In general, an advantage of this method is that the seven degree-of-freedom robot can be paired easily with a variety of spatula designs, and the dispensing motion easily adapted to the specific design.

Fig. 2 Spatulas that were custom-designed to be used by the dual-armed robot (from left to right; large, medium, small spatulas).

An analytical balance‖ with a sliding door was chosen to obtain better and more consistent weighing results. The only physical modification is a custom glass closure with a robot-friendly shaped handle. A matching funnel holder and

§ Designing model is listed in ESI section.†

¶ The value is approximate for tested solid, density matters.

‖ Ohaus Pioneer PX523/E.

a positioning pin for the solid storage hopper are placed on the top layer of the balance enclosure.

A detailed demonstration video that shows the robot carrying out a complete solid dispensing protocol is provided in the Data availability section.

2.3 Autonomous robotic solid dispensing

Our autonomous solid dispensing approach involves the robot executing a solid dispensing algorithm, with a closed-loop fuzzy logic controller to manage the solid transfer. The Algorithm 1 can be summarized as follows: first, the algorithm selects the appropriate spatula size for scooping the solid from its hopper, based on the amount that remains to be dispensed. This mimics the traditional human approach, where a smaller spatula might be selected as the target weight is approached. A fuzzy logic controller is used to govern the shaking frequency and the tilting angle of the dispensing spatula, again based on the difference between the target weight and the current weight, also factoring in a measure of the particle size or granularity. To elaborate the details of the algorithm for autonomous robotic solid dispensing:

Algorithm 1: Automatic Solid Dispensing Algorithm

Input: W_t, S_p
$W_c = 0$
$\Delta W = W_t - W_c$
prepare_workspace()
keep_dispensing = True
/* Solid dispensing starts */
while *keep_dispensing = True* **do**
  if $\Delta W \geq W\_max\_l$ **then**
    select_large_spoon()
  else if $W\_max\_l \geq \Delta W$ *and* $\Delta W \geq W\_max\_m$ **then**
    select_medium_spoon()
  else
    select_small_spoon()
  end
  scoop()
  do
    $W_p = W_c$
    dispense_solid($\Delta W, S_p$)
    $\Delta W = W_t - W_c$
    if $\Delta W > \varepsilon_c$ **then**
      restart()
    else if $|\Delta W| \leq \varepsilon_t$ **then**
      keep_dispensing = False
      break
    else
      $\Delta C = |W_c - W_p|$
    end
  while $\Delta C > \varepsilon_c$
end

(1) The target dispense weight (W_t) and solid particle size (see below) (S_p) are provided as inputs to the algorithm.

(2) The current dispensed weight (W_c) is initially zero. Thereafter, the difference between the target weight and the current weight (ΔW) is calculated.

(3) Before beginning the dispensing process, the robot performs a number of preparatory steps that include: (i) opening the balance door; (ii) moving the receiving vial to the balance pan; (iii) closing the balance door; (iv) moving the hopper containing the solid to be dispensed to the dispensing location (this is designed such that the travel distance between the hopper and the receiving vial is minimized), and; (v) finally, mixing the solid in the hopper using a spatula to guarantee a uniform distribution of the solid.

(4) To begin the dispensing process, the flag (*keep_dispensing*) is set to true, where the process will continue as long as this flag is set.

(5) Depending on the amount that needs to be dispensed, an appropriate spatula is selected. Three spoon sizes are available; large, medium, and small. The large spatula is used to dispense amounts larger than 0.8 g (*W_max_l*), the medium spatula is used for dispensing amounts from 0.1 g (*W_max_m*) to 0.8 g and the smallest spatula is for amount smaller than 0.1 g. Accordingly, the error ΔW is used to determine the appropriate spoon for the robot to pick up.

(6) After picking up the appropriate spatula, the robot uses a scooping motion to pick solid from the hopper.

(7) In preparation for dispensing, pre-dispensing weight (W_p) is first recorded. The robot then moves the spoon to a funnel that delivers the solid into the receiving vial, and carries out a dispensing episode using the fuzzy logic controller based on the given particle size S_p, the difference between target weight and current weight ΔW to control the dispensing motion. This controller will be further described in the next section.

(8) After completing a dispensing episode, the currently dispensed weight W_c is updated and the error ΔW is recalculated. If the error is within the acceptable dispense tolerance (e_t), then the dispensing process is complete, and the flag *keep_dispensing* is set to false. The dispensing process is then deemed successful. If the error is larger than e_t, then the whole algorithm is restarted. Specifically, the robot places the spatula down after emptying its contents into the solid hopper. It then opens the balance door, picks up the receiving vial, and pours its contents back into the hopper. The algorithm is then started again from the beginning.

(9) If the error is less than the tolerance, then the change between two consecutive dispenses (ΔC) is calculated. This change is used to determine whether there is enough solid left in the spoon to carry out to the next dispensing episode or, if no solid is left in the spatula, there is a need to change the spatula size and scoop again. Specifically, if ΔC is bigger than the dispense change tolerance (e_c), then next dispense episode can be carried out. Otherwise, the algorithm goes back to the spatula selection step.

The ability to check for over-dispensing and to restart the dispensing process goes beyond what is available in current commercial dispensing platforms. This is possible because we use a versatile dual-armed robot that can manipulate the balance door, the solid hoppers, the receiving vials, and the spatulas.

2.4 Solid dispensing fuzzy logic controller

2.4.1 Fuzzy logic control. Fuzzy logic control (FLC) is a control strategy that uses the fuzzy set theory. FLC represents

Table 1 Relationship between particle size range and FLC input level

Actual particle size (μm)	Level
0–0.1	1
0.1–1	2
1–10	3
10–500	4
Else, size = coarse	5

Table 2 Particle size levels for the tested solid materials

Material	Particle size (μm)	Level
Al_2O_3	0.55 ± 0.45	2
$CaCO_3$	6 ± 4	3
Na_2SO_3	63 ± 27	4
$NaNO_2$	115 ± 85	4
CH_3COOK	100 ± 50	4
Pectin	120 ± 80	4
Sand	275 ± 125	4
SiC	240 ± 160	4
Granulated sugar	300 ± 100	4
$NH_4CH_3CO_2$	250 ± 50	4
Activated carbon	650 ± 250	5
$LiOH \cdot H_2O$	450 ± 350	5
Molecular sieve	2500 ± 500	5

a problem as a sequence of IF-ELSE conditional statements. These statements are combined using membership degree functions, which represent their outputs as a probability of events occurring rather than traditional Boolean 0 or 1 values.[13,14]

FLCs are used extensively in non-linear real-world control systems as they can incorporate human experience. They are also more robust than traditional controllers because they can allow complex systems to be modelled where mathematical representations may not be possible.[13,14]

Our fuzzy controller system structure is shown in Fig. 5. The main components of such a system are: fuzzification, inference engine and defuzzification.[15,16] Fuzzification is the process of converting the deterministic input values into their corresponding fuzzy set counterparts. This converts the discrete numerical inputs into fuzzy sets or variables. Defuzzification is the inverse, where fuzzy variables are converted back into their actual numerical values. Both conversion steps are achieved using membership degree functions. In the inference step, rules that govern the process to be controlled are described using IF-ELSE statements and are stored in a rule base. These rules are then applied to the input fuzzy variables such that the output from each rule is deduced using the inference engine. The values of these outputs are described using fuzzy variables or sets. In the end, the discrete numerical output value for these outputs is obtained in the defuzzification step by combining them using any of the membership functions combination methods, such as fuzzy centroids.[13–16]

2.4.2 Solid dispensing controller design. In the formulation of this solid dispensing problem, the FLC operate by varying the spatula tilt angle and the shaking routine, based on certain inputs.

Two FLCs are utilised in our method to control the solid dispensing process. There is no controller for large spatula, robot will transfer all solid from large spatula to vials.

(1) FLC1 controls the shaking motion for the medium-sized spatula, which takes two inputs; the particle size level and the difference between the dispensed weight and the target weight.

(2) FLC2 controls small spatula tilt angle and takes the same inputs as FLC1.

The particle size level for each solid is classified into five categories in accordance with experimental measurements (Table 1). Both the particle size and the corresponding particle size level are illustrated in Table 2. The actual particle size is measured by SEM (scanning electron microscopy).** We note that although SEM is used for classification here, our results suggest that a simple visual, empirical grading (*e.g.*, fine to coarse, 1–5) could also be employed.

Our FLC system architecture is shown in Fig. 5. It contains the following components: fuzzification, inference engine, and defuzzification.[15,16] The binary output value is obtained by computing from 'fuzzy centroid' of the composite region of the output membership functions.[13–16]

Trapezoidal membership functions are used for both input and output membership functions in the fuzzification process. These membership functions are selected because of their robustness in representing various values and they are commonly used in the literature.[17,18] The Mamdani type inference minimum function, also known as the max–min inference method, is employed for the inference step[15] because this provides improved interpretability when using the rule base.[19]

FLC1 is considered to be a system with two inputs and one output. The membership function for input 1 – particle size (Fig. 3 left) – comprises two trapezoidal functions with two variables (small, large). The membership function for input 2 – difference (Fig. 3 medium) – includes three linguistic variables over the range of 0.1 g to 0.8 g (small, medium, large). The output of the FLC (Fig. 3 right) includes three levels (small, medium, large), ranging over 0–10 shaking times. The rule base†† consisted of 6 possibilities (3 difference × 2 particle size) of the medium spoon fuzzy controller.

Similarly, FLC2 is a two-input, one-output system. The input 1 – particle size level membership function – is the same as for FLC1. Input 2 – the different membership function (Fig. 4) – comprises five fuzzy regions representing the linguistic variables (VS, S, M, L, VL) over the dispensing range less than 0.1 g. The output spatula tilt angle membership function (Fig. 4 right) corresponds to five variables (VS, S, M, L, VL) ranging over 40–60 degrees from the horizontal. The rule base therefore includes rules with 10 possibilities (5 difference × 2 particle size) for FLC2.

After the Mamdani inference, a mapping from an input to an output is formulated, and de-fuzzification is performed to

** Images and instrument information are provided in ESI section.†

†† The rule base table is provided in ESI section.†

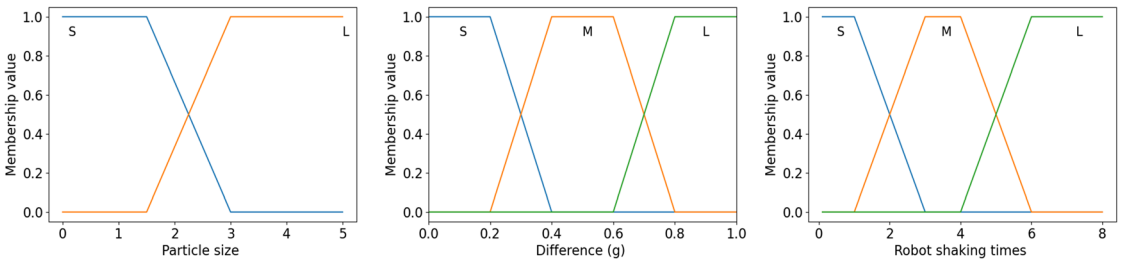

Fig. 3 Input 1, input 2 and output membership function for FLC1/medium spatula (left to right).

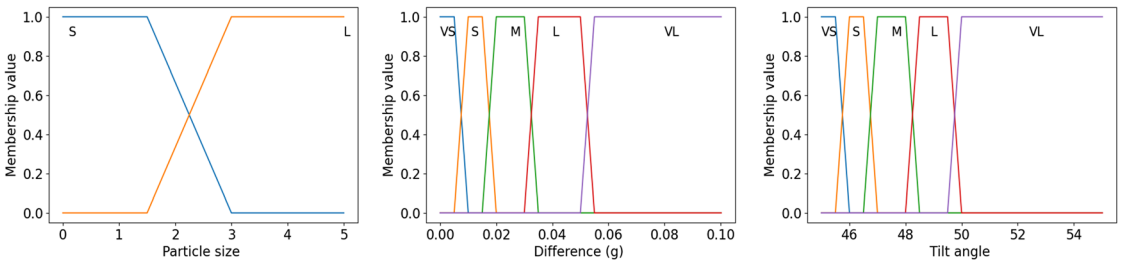

Fig. 4 Input 1, input 2 and output membership function for FLC2/small spatula (left to right).

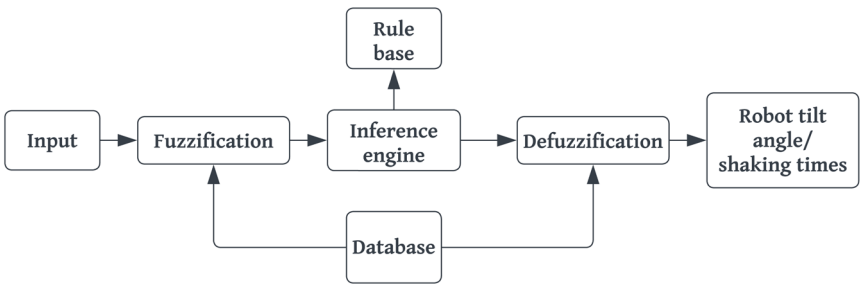

Fig. 5 Process for the fuzzy logic controller.

convert fuzzy variables into binary values using the centre of gravity method. This process performed de-fuzzification by finding the centre of the area encompassed by all the rules, and is mathematically described by the following formula:[15]

$$\mu(t) = \frac{\sum_{i=1}^{n} \mu_i \mu_v(\mu_i)}{\sum_{i=1}^{n} \mu_v(\mu_i)} \quad (1)$$

where $\mu(t)$ refers to the defuzzification output, μ_i refers to the output variable and μ_v represented the aggregated membership function. The defuzzification outputs are robot shaking time and spatula tilt angle for FLC1 and FLC2, respectively.

3 Experimental

We benchmarked our solid dispensing platform against two commercial platforms for a range of different solids. These performance tests were designed to evaluate generality based on solid type, as well as accuracy and precision. The biomimetic approach performed well in both respects, especially when one considers that this was a prototype device and not a full commercial implementation.

3.1 Benchmarking platforms

We benchmarked against two commercial solid dispensing systems: the Chemspeed gravimetric dispensing unit for fine powder dosing (GDU-Pfd) and the Quantos (Mettler Toledo XPE206 dosing system‡‡). We have had significant prior experience in our labs with both of these platforms.[2]

3.2 Methodology

Four target weights§§ were chosen spanning the range 20 mg to 1 g, which covers a significant percentage of laboratory scale work. For each material, dispensing of each target weight was attempted 30 times. The percentage weighing error was used a one metric to evaluate platform performance. This was

‡‡ Layout of both commercial dispensing systems are listed in ESI.†

§§ Except for the solid-molecular sieve material, where the large particle size meant that only three target weights were chosen.

Table 3 Different solids tested in the experiment

Material	Absorption%	Bulk density (g cm^{-3})	Mohs' hardness
Al_2O_3	0.05	3.97 (ref. 24)	8–9 (ref. 25)
$CaCO_3$	0.05	2.03	3 (ref. 26)
Na_2SO_3	0.10	2.63 (ref. 27)	—
$NaNO_2$	0.95	2.168	—
CH_3COOK	33.45	1.6 (ref. 28)	—
Pectin	8.32	0.96 (ref. 29)	—
Sand	0.19	1.63 (ref. 30)	7 (ref. 11)
SiC	0.15	3.21 (ref. 31)	9–9.5 (ref. 32)
Granulated sugar	0.50	0.7 (ref. 33)	—
$NH_4CH_3CO_2$	26.60	1.17 (ref. 34)	—
Activated carbon	6.10	1.48 (ref. 35)	—
$LiOH \cdot H_2O$	44.77	1.51 (ref. 36)	—
Molecular sieve	5.21	—	—

defined as the difference between the dispensed mass and the target mass, divided by the target mass:[9]

$$\frac{(\text{mass dispensed} - \text{target mass})}{\text{target mass}} \times 100 = \text{error}\% \quad (2)$$

3.3 Material

To reduce measurement errors, all solids were dried in an oven at 115 °C for 6 hours before dispensing.

Table 3 listed the thirteen different solids used in these benchmark tests, chosen to include inorganic materials, organic materials, and a wide range of particle sizes, abrasive materials (*e.g.*, sand, SiC) were also included.[12,20–22]

We also considered three characteristics for these solids; the water absorption%, the bulk density, and the Mohs' hardness. The absorption% is expressed as the water uptake (M) per unit weight of absorbent solid.¶¶ The water uptake (M) of each solid was calculated as:[23]

$$M = \frac{m - m_o}{m_o} \quad (3)$$

where m referred to the mass of solid with absorbed moisture and m_o is the oven-dried solid mass. As was clear from Table 3, the solids spanned a wide range of water affinities, ranging from organic salts such as potassium acetate, which absorb large amounts of moisture to materials and aluminium oxide, which absorbed very little water.

Table 3 also gave bulk densities and hardness values for selected solids, where they have been reported in the literature.

4 Results

4.1 Dispensing performance

We first analysed how our platform against the two benchmarked commercial systems in terms of solid-dispensing accuracy over a range of masses.

¶¶ For these tests, the specific moisture and dried mass, humidity and temperature records were recorded and were available in ESI section.†

Fig. 6 and Table 6 showed the accuracy of dispensing thirteen materials across the three platforms. Note that the average results in Table 6 included all dispensing failures, which can cause a 100% error (that is, the solid was not dispensed).

A primary evaluation metric was the percentage weighing error at the three different target weights for the 13 different materials. A positive percentage error represented over-dispensing or overshooting above the target weight, while a negative error represents under-dispensing. For some solids, relatively large over-dispensing errors were observed periodically when using both the Quantos and the Chemspeed automated gravimetric solid dosing. This was mainly caused by the dosing head on the Quantos or Chemspeed dispensing cartridges failing to close, perhaps because of a partially blocked dispensing mechanism. We note that this was not consistently the case; for example, in the case of dispensing sugar at 1000 mg scale using the Chemspeed platform, there were two significant over-dispenses (67.0% and 85.5% error over-dispensed), while the other 28 dispenses were very close to the target weight (0.2% error). For other materials (*e.g.*, sand at 50 mg target dispense using the Quantos system), over-dispensing was much more common because of the coarse nature of the material, which is not very compatible with the Quantos dispensing heads. To summarize the overall performance of the three platforms across the 13 materials, we considered the percentage dispensing error at a 200 mg target scale for (i) the 'non-challenging' solids and (ii) for all 13 solids. As summarized in Table 5, our biomimetic robot approach performed better on average than the two benchmark systems for the non-challenging solids at this scale. When the challenging solids were considered, some of which did not dispense at all (see Fig. 6), then the average percentage error was much higher and approximately the same for all three systems.

There were a number of solids where frequent failures occurred during dispensing; failure means that a single dispensing procedure was not completed. Table 7 and Fig. 6 summarize these failure rates. Solids with more than a 10% failure rate across all the runs were considered as 'challenging solids' for the corresponding dispensing platform.

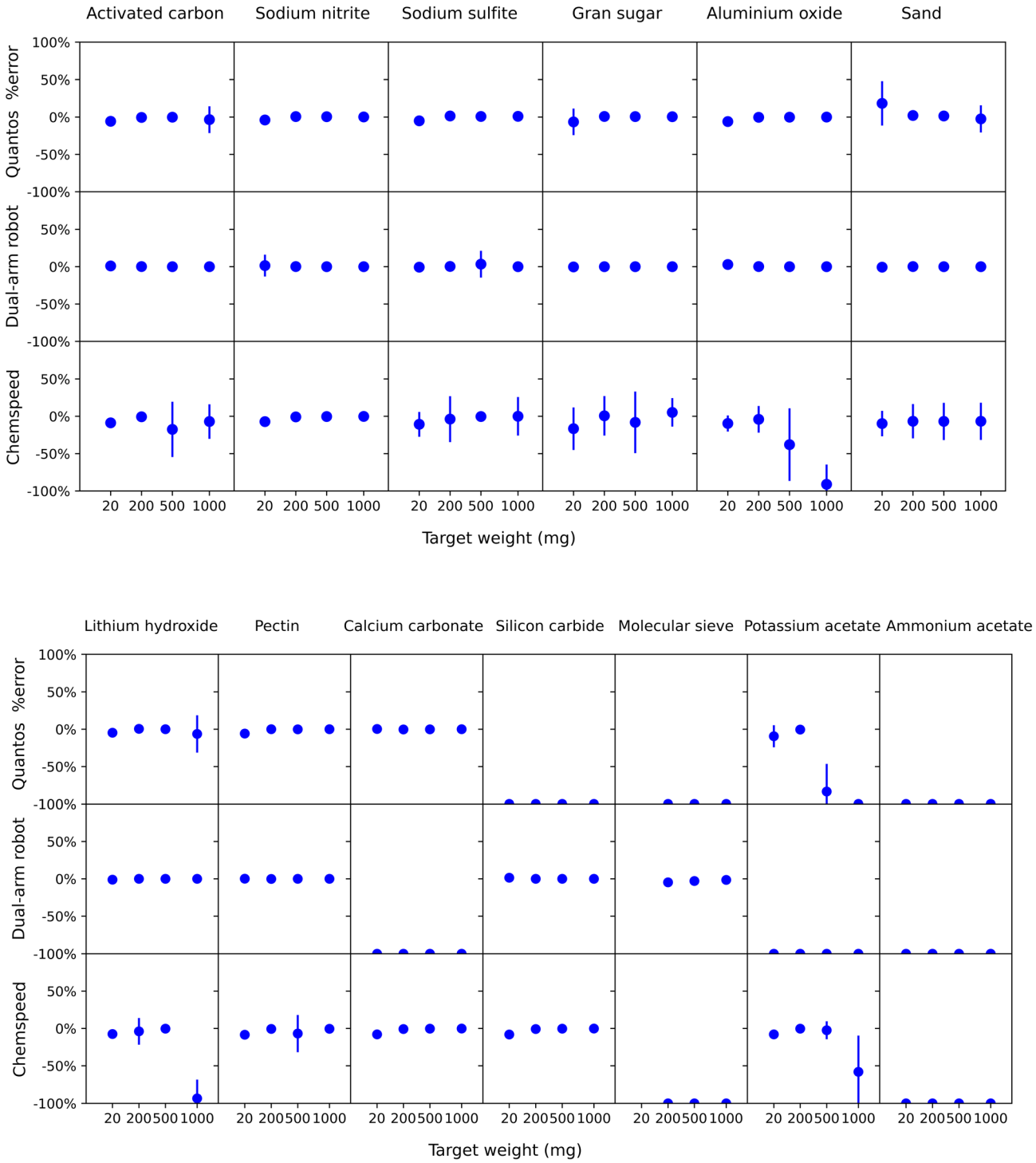

Fig. 6 Comparison between the different dispensing methods plotting average percentage dispensing error (see eqn (2)) with standard deviation for thirteen different solids with different target dispensing weights. Each row of sub-figures represents the data from a different dispensing platform, while each column represents a different solid. −100% dispensing indicates total failure to dispense the solid, most commonly because of a blockage.

Table 4 Comparison of the dispensing time (seconds) for sodium nitrite dispensing on the three platforms with 2 mg tolerance

Target weight (mg)	Dual-arm robot	Quantos	Chemspeed
1000	552 ± 128	40 ± 4	134 ± 17
500	517 ± 72	33 ± 2	132 ± 21
200	381 ± 73	31 ± 3	109 ± 19
20	239 ± 30	285 ± 2	62 ± 23

These dispensing failures were due primarily to either: (1) failure of the dispensing mechanism (*i.e.*, typically, blockage of the cartridge used in the Chemspeed, the dosing head used in the Quantos, or the funnel used in our dual-arm robotic method); (2) the solid was too abrasive, resulting in a failure of the moving parts in the cartridge or dosing head which applied to Chemspeed and Quantos; (3) a robot manipulation error (for our new system only).

As detailed in Table 7, different solids were 'challenging' for different platforms. For the Chemspeed platform, the most challenging solids were molecular sieves, ammonium acetate, potassium acetate, lithium hydroxide monohydrate, and aluminium oxide. However, the Chemspeed system also performed poorly when dispensing sugar, as shown in Fig. 6.

For the Quantos platform, the challenging solids included potassium acetate, molecular sieves and ammonium acetate. Also, silicon carbide and sand proved extremely challenging for the Quantos platform because they are highly abrasive.

For the dual-arm robot platform, the challenging solids were calcium carbonate, potassium acetate, and ammonium acetate due to the compressibility ($CaCO_3$) or hygroscopic properties ($NH_4CH_3CO_2$ and CH_3COOK) that can cause solids to stick on the inside of funnels and spatulas; in some cases, this caused the funnel to be blocked.

Overall, these data suggested that the new robotic platform might be more versatile than the two benchmarking systems, with the exception of hygroscopic, deliquescent and compressible materials where funnel blockage was observed, at least in this first prototype design.

Table 5 lists the average percentage error which was the evaluation metric, across the different platforms and for all the thirteen materials.

For non-challenging solids, the percentage error was less than 2% for the Quantos system and the dual-arm robot. The average error for these solids was just 0.07% for the dual-arm robot at this 200 mg scale. For the Chemspeed platform, the average percentage error was higher because two failures (out of 30 dispenses) with 100% error occurred in the dispensing of granulated sugar. Failures were caused by failing to finish the closing and opening operation of the dispensing mechanism.

The dispensing time was also measured for sodium nitrite for all three platforms under different target values with 2 mg tolerance and the results are listed in Table 4. We note that the dispensing time was affected by the characteristics of the solid, the target weight, and the tolerance. Compared with the two commercial platforms, the dispensing time on our dual-arm robot platform was significantly longer, particularly when compared to the Quantos system. This was because of the time required to manipulate more tools (vials, hoppers, scales doors and different sized spatulas). Also, in cases where the dispensing restarts to correct over-dispensing, this significantly added to the average dispensing time. As such, there was a trade-off between the dispensing time and the target precision.

4.2 Failure analysis

Failure in the dispensing process was defined as the non-completion of a single dispensing procedure. Table 7 summarizes the number of failures over 120 runs for all the thirteen materials previously described.

Note that for the molecular sieve only 90 runs were carried out because it was not possible to test the lowest target weight due to the large size of the particles. Table 7 describes the cause of failures. There were three main reasons for failures: mechanical, solid deliquescing and robotic errors.

Mechanical failures in the Quantos and Chemspeed (GDU-Pfd) platforms were due to problems with the closing and opening operation of the dispensing mechanism, in terms of our robotic platform, it was either because the funnel or the spatula outlet became blocked. With the most abrasive materials, silicon carbon, the Quantos dispensing heads were damaged irreparably.

Likewise, deliquescent solids of led to material being stuck to the inner walls of dispensing mechanism, *i.e.*, the dispensing head for the Quantos, the dispensing cartridge for Chemspeed, and the dispensing spatula for dual-arm robotic platform. As a result, the solid failed to be dispensed into the vial. In principle, this might be solved by operating the platform in a dry environment for such materials.

Finally, for the dual-arm robotic platform, a robot error could occur when the program detected there was no change on the balance during continuous dispensing. This was

Table 5 Percentage solid dispensing error result at a 200 mg target scale on three platforms

	Quantos	Dual-arm robot	Chemspeed
Non-challenging solids	−0.41% ± 1.80%	0.07% ± 0.56%[a]	−2.23% ± 12.39%
All solids	−23.39% ± 1.58%	−22.85% ± 0.82%	−17.39% ± 11.98%

[a] These tabulated results do not include the solid molecular sieve where the average weight of each sieve particle is 5–10 mg.

Table 6 Comparison of different dispensing methods and the percentage dispensing error for thirteen solids with different target dispensing weights

		Error%		
Material	Target weight (mg)	Quantos	Dual-arm robot	Chemspeed
Al_2O_3	1000	−0.02 ± 0.05	0.06 ± 0.10	−91.01 ± 26.39
	500	−0.15 ± 0.09	0.05 ± 0.18	−37.92 ± 48.67
	200	−0.32 ± 0.11	0.08 ± 0.52	−4.02 ± 17.83
	20	−6.00 ± 0.93	3.00 ± 5.42	−9.60 ± 10.81
$CaCO_3$	1000	−0.00 ± 0.12	−100.00 ± 0.00	−0.18 ± 0.04
	500	−0.15 ± 0.05	−100.00 ± 0.00	−0.34 ± 0.10
	200	−0.30 ± 0.13	−100.00 ± 0.00	−0.80 ± 0.28
	20	0.40 ± 0.45	−100.00 ± 0.00	−7.88 ± 2.39
Na_2SO_3	1000	1.02 ± 1.07	0.06 ± 0.10	−7.04 ± 23.08
	500	0.77 ± 0.69	3.35 ± 17.95	−17.49 ± 37.01
	200	1.39 ± 1.63	0.27 ± 0.46	−0.69 ± 0.30
	20	−5.04 ± 1.78	−0.67 ± 6.02	−8.78 ± 1.70
$NaNO_2$	1000	0.16 ± 0.17	0.04 ± 0.11	0.09 ± 0.24
	500	0.45 ± 0.28	0.01 ± 0.16	−0.34 ± 0.09
	200	0.67 ± 0.80	0.22 ± 0.51	−0.81 ± 0.42
	20	−3.96 ± 2.40	1.50 ± 14.61	−7.10 ± 5.41
CH_3COOK	1000	100.00 ± 0.00	−100.00 ± 0.00	−58.04 ± 48.45
	500	83.20 ± 37.58	−100.00 ± 0.00	−2.42 ± 12.07
	200	−0.45 ± 1.32	−100.00 ± 0.00	−0.30 ± 0.98
	20	−9.45 ± 14.77	−100.00 ± 0.00	−8.02 ± 3.29
Pectin	1000	−0.01 ± 0.10	−0.04 ± 0.06	−0.41 ± 1.30
	500	−0.09 ± 0.11	−0.03 ± 0.15	−6.88 ± 24.89
	200	−0.07 ± 0.26	−0.23 ± 0.28	−0.70 ± 0.61
	20	−5.87 ± 1.37	0.16 ± 3.53	−8.50 ± 1.35
Sand	1000	−2.47 ± 18.15	0.02 ± 0.10	−6.73 ± 244.93
	500	1.54 ± 1.1.4	0.07 ± 0.22	−6.88 ± 24.89
	200	−2.12 ± 1.34	0.15 ± 0.56	−6.61 ± 22.97
	20	18.35 ± 29.64	0.67 ± 6.15	−9.73 ± 17.09
SiC	1000	−100.00 ± 0.00	0.00 ± 0.09	−0.17 ± 0.09
	500	−100.00 ± 0.00	0.02 ± 0.25	−0.34 ± 0.07
	200	−100.00 ± 0.00	−0.07 ± 1.05	−8.20 ± 0.17
	20	−100.00 ± 0.00	1.50 ± 4.50	−8.13 ± 1.06
Granulated sugar	1000	0.55 ± 0.29	−0.02 ± 0.08	5.26 ± 19.12
	500	0.73 ± 0.52	−0.01 ± 0.21	−8.15 ± 41.25
	200	0.85 ± 1.20	0.07 ± 0.42	0.68 ± 26.45
	20	−6.42 ± 17.74	−0.34 ± 4.27	−16.63 ± 28.45
$NH_4CH_3CO_2$	1000	−100.00 ± 0.00	−100.00 ± 0.00	−100.00 ± 0.00
	500	−100.00 ± 0.00	−100.00 ± 0.00	−100.00 ± 0.00
	200	−100.00 ± 0.00	−100.00 ± 0.00	−100.00 ± 0.00
	20	−100.00 ± 0.00	−100.00 ± 0.00	−100.00 ± 0.00
Activated carbon	1000	−3.45 ± 17.93	0.01 ± 0.10	−7.04 ± 23.08
	500	−0.20 ± 0.14	0.04 ± 0.20	−17.49 ± 37.01
	200	−0.53 ± 0.24	0.15 ± 0.50	−0.69 ± 0.31
	20	−5.62 ± 1.65	1.00 ± 4.73	−8.78 ± 1.70
$LiOH \cdot H_2O$	1000	−6.32 ± 25.06	0.01 ± 0.12	−93.35 ± 24.89
	500	−0.02 ± 0.29	0.07 ± 0.21	−0.30 ± 0.08
	200	−0.46 ± 0.56	0.00 ± 0.45	−3.91 ± 17.85
	20	−4.76 ± 19.50	−1.17 ± 1.02	−7.42 ± 3.10
Molecular sieve	1000	−100.00 ± 0.00	−1.51 ± 0.38	−100.00 ± 0.00
	500	−100.00 ± 0.00	−2.93 ± 0.76	−100.00 ± 0.00
	200	−100.00 ± 0.00	−4.75 ± 5.45	−100.00 ± 0.00

typically caused by a compressible solid clogging up the spatula outlet.

4.3 Discussion

To assess the overall performance of the three different platforms, three metrics were considered. These were the ability to dispense a large range of solids, the percentage error when dispensing, and the dispensing time. The dual-arm robot and the Quantos platform were able to dispense a wider range of solids than the Chemspeed, as shown in Table 7, at least within the range of solids that we trialled here. Challenging solids for the dual-arm robotic platform were compressible powder materials such as calcium carbonate and highly hygroscopic solids such as potassium acetate and ammonium

Table 7 Comparison of different dispensing methods and the percentage dispensing failure rate (%) for all solids

Material	Dual-arm robot	Quantos	Chemspeed
Al_2O_3	0	0	31.7[a]
$CaCO_3$	100[a]	0	0
Na_2SO_3	0.8[c]	0	4.2[a]
$NaNO_2$	0	0	0
CH_3COOK	100[b]	45.8[b]	14.2[b]
Pectin	0	0	1.7[a]
Sand	0	1.7[a]	55.8[a]
SiC	0	100[a]	0
Granulated sugar	0	0	8.3[a]
$NH_4CH_3CO_2$	100[b]	100[b]	100[b]
Activated carbon	0	0.8[a]	4.2[a]
$LiOH \cdot H_2O$	0	1.7[a]	24.2[a]
Molecular sieve	0	100[a]	100[a]
All solids (average)	23.1	26.9	26.5

[a] Mechanical failure. [b] Solid deliquescing. [c] Robot reporting error.

acetate. For the Quantos platform, the challenging solids included abrasive materials such as silicon carbide with high hardness, as well as certain hygroscopic materials and large granule solids, such as molecular sieve. The Chemspeed platform showed a different set of characteristics; for example, abrasive silicon carbide was dispensed effectively, while sand and Al_2O_3 were not.

From these tests, it appeared that the main advantages of using a dual-arm robot for solid dispensing stems from its ability to dispense a wider range of materials including abrasive materials and solids with large particles. It was also more precise (Table 5) for non-challenging solids, albeit at the expense of speed (Table 4). This speed disadvantage, however, may be counterbalanced in some applications by versatility, precision, and the ability to restart the dispensing process if high absolute precision is needed. Moreover, it was possible that the dual-arm robot could also be used for other tasks in autonomous workflows, such as capping and decapping vials.[2,37]

5 Conclusions

We have developed a unique automated solid dispensing platform using a dual-arm robot that uses a human-like dispensing method. This approach provides a flexible and relatively inexpensive platform for solid dispensing that can accelerate automated chemistry workflows in the future. These benefits stem from the versatility and increasing commoditization of consumer robots such as the ABB YuMi platform, and it further highlights their potential for automating chemical workflows in laboratories.

This method has certain advantages over current commercial dispensing platforms for widening the range of dispensable solids, particularly for larger particles and abrasive solids dispensing. However, compressible fine powders and hygroscopic solids can pose problems for our method, and dispensing fails for some solids with the current configuration. Longer dispensing times are also a drawback, but this is counterbalanced by versatility, improved precision and potentially increased automation.

Future work will include technical improvements to the platform as well as its use in research applications. We envisage improved dispensing algorithms that incorporate self-learning for specific solids; it might also be feasible to incorporate visual feedback to augment the feedback from the analytical balance. This solid dispensing workstation is modular and could be extended by connecting it to other stations. For example, a mobile robot[2] could be used to deliver additional empty vials to the station and to transport filled vials to other stations, such as a chemical synthesis station. We will also exploit the versatility of the dual-arm robot to incorporate other tasks into workflows beside solid dispensing. As an example, the dual-arm robot might double as a capping/decapping station for sample vials. Thinking more broadly, these results suggest that other biomimetic approaches could be developed where robots use relatively simply tools to reproduce, more or less, the operations carried out by human researchers, rather than building more bespoke automated laboratory devices.

Data availability

ESI† including codes, models and dispensing results have been uploaded to **https://github.com/fourteenjiang/Solid-dispensing.git**. A detailed demonstration video can be found at **https://doi.org/10.5281/zenodo.8082246**.

Conflicts of interest

There are no conflicts to declare.

Note added in proof

For context, we did not examine the entire range of products offered by Chemspeed or Mettler-Toledo for solid dispensing and we focused on tools that we had ready access to. Alternative tools do exist; for example, for dispensing sub-milligram quantities of solids, which our robotic system cannot achieve, and larger dispensing cartridges to handle bigger particles and larger quantities of solid. Likewise, these manufacturers offer the ability to manually calibrate dispensing for specific solids, at some expense of autonomy, which can further improve dispensing precision.

Notes and references

1 A. M. Fermier, J. Troisi, E. C. Heritage, M. A. Drexel, P. Gallea and K. A. Swinney, *Analyst*, 2003, **128**, 790–795.
2 B. Burger, P. M. Maffettone, V. V. Gusev, C. M. Aitchison, Y. Bai, X. Wang, X. Li, B. M. Alston, B. Li, R. Clowes, *et al.*, *Nature*, 2020, **583**, 237–241.
3 M. Christensen, L. P. Yunker, P. Shiri, T. Zepel, P. L. Prieto, S. Grunert, F. Bork and J. E. Hein, *Chem. Sci.*, 2021, **12**, 15473–15490.
4 M. Li, X. Tian and X. Chen, *Biofabrication*, 2009, **1**, 032001.

5 A. Aspuru-Guzik and K. Persson, *Mission Innovation*, 2018.
6 S. K.-F. Wong, Y. Lu, W. Heineman, J. Palmer and C. Courtney, *J. Biomol. Screening*, 2005, **10**, 524–531.
7 M. N. Bahr, M. A. Morris, N. P. Tu and A. Nandkeolyar, *Org. Process Res. Dev.*, 2020, **24**, 2752–2761.
8 S. A. Biyani, Y. W. Moriuchi and D. H. Thompson, *Chem.: Methods*, 2021, **1**, 323–339.
9 M. C. Martin, G. M. Goshu, J. R. Hartnell, C. D. Morris, Y. Wang and N. P. Tu, *Org. Process Res. Dev.*, 2019, **23**, 1900–1907.
10 A. B. Santanilla and G. Cook, The Power of High-Throughput Experimentation: Case Studies from Drug Discovery, *Drug Development, and Catalyst Discovery*, ACS Publications, 2022, vol. 2, pp. 3–21.
11 N. Will, M. Vitt, A. Goerke, M. Loebering, J. Laukart, M. Baehr and C. Langebrake, *Eur. J. Hosp. Pharm.*, 2016, **23**, A213.
12 M. N. Bahr, D. B. Damon, S. D. Yates, A. S. Chin, J. D. Christopher, S. Cromer, N. Perrotto, J. Quiroz and V. Rosso, *Org. Process Res. Dev.*, 2018, **22**, 1500–1508.
13 P. Albertos, A. Sala and M. Olivares, *Proc. Congreso Español sobre Tecnologías y Lógica Fuzzy*, 2000, pp. 1–11.
14 J. L. Castro, *IEEE Trans. Syst. Man Cybern.*, 1995, **25**, 629–635.
15 M. Singh, P. Kumar and I. Kar, *IEEE Trans. Smart Grid*, 2012, **3**, 565–577.
16 L. Behera and I. Kar, *Intelligent systems and control principles and applications*, Oxford University Press, Inc., 2010.
17 O. Kosheleva and V. Kreinovich, *International Conference on Information Processing and Management of Uncertainty in Knowledge-Based Systems*, 2018, pp. 127–138.
18 O. Kosheleva, V. Kreinovich and S. Shahbazova, *Recent Developments and the New Direction in Soft-Computing Foundations and Applications*, Springer, 2021, pp. 63–75.
19 J. Galindo, *Handbook of Research on Fuzzy Information Processing in Databases*, IGI Global, 2008.
20 S. Yang and J. Evans, *Powder Technol.*, 2007, **178**, 56–72.
21 G. Rovero, M. Curti and G. Cavaglià, *Adv. Chem. Eng.*, 2012, 404–434.
22 J. J. Beaman, J. W. Barlow, D. L. Bourell, R. H. Crawford, H. L. Marcus and K. P. McAlea, *Solid freeform fabrication: a new direction in manufacturing*, 1997, vol. 2061, 25–49.
23 R. Liu, T. Gong, K. Zhang and C. Lee, *Sci. Rep.*, 2017, **7**, 1–9.
24 D. R. Lide, *CRC Handbook of Chemistry and Physics*, CRC press, 2004, vol. 85.
25 L. Peña-Parás, J. Taha-Tijerina, L. Garza, D. Maldonado-Cortés, R. Michalczewski and C. Lapray, *Wear*, 2015, **332**, 1256–1261.
26 J. Park, J. Gweon, H. Seo, W. Song, D. Lee, J. Choi, Y. C. Kim and H. Jang, *Tribol. Int.*, 2022, **165**, 107334.
27 CAMEO Chemicals, *Sodium Sulfite*, **https://cameochemicals.noaa.gov/chemical/12645**, 1992.
28 ILO International Chemical Safety Cards, *Potassium Acetate*, **https://www.ilo.org/dyn/icsc/showcard.display?p_version=2&p_card_id=0547**, 2006.
29 Pectin, *Density of Pectin, Liquid (Food)*, **https://www.aqua-calc.com/page/density-table/substance/pectin-coma-and-blank-liquid**.
30 Sand, *Density of Sand, Dry (Material)*, **https://www.aqua-calc.com/page/density-table/substance/sand-coma-and-blank-dry**.
31 B. J. Baliga, *Wide Bandgap Semiconductor Power Devices: Materials, Physics, Design, and Applications*, Woodhead Publishing, 2018.
32 H. Lee, D. Kim, J. An, H. Lee, K. Kim and H. Jeong, *CIRP Ann.*, 2010, **59**, 333–336.
33 Density of Sugar Factory Products, *The Sugar Engineers*, **https://www.sugartech.co.za/density/index.php**.
34 R. C. Weast, M. J. Astle and W. Beyer, Physical constants of organic compounds, *H.Crc Handbook of Chemistry and Physics*, 1988, vol. 3, pp. 178–576.
35 Density of Activated Carbon (Material), *Activated Carbon*, **https://www.aqua-calc.com/page/density-table/substance/activated-blank-carbon**.
36 ILO International Chemical Safety Cards (ICSC), *Lithium Hydroxide Monohydrate*, **https://www.ilo.org/dyn/icsc/showcard.display?p_version=2&p_card_id=0914**.
37 K. Junge, J. Hughes, T. G. Thuruthel and F. Iida, *IEEE Robot. Autom. Lett.*, 2020, **5**, 760–765.